

ORIGINAL ARTICLE

Satellite Laser Ranging technique as a tool for the determination of the Schwarzschild, de Sitter and Lense-Thirring effects

Mateusz Matyszewski^{1*}, Paweł Lejba¹, Marcin Jagoda² and Paweł Tysiąg³

¹Space Research Centre, Polish Academy of Sciences, Bartycka 18A, 00-716 Warsaw, Poland

²Faculty of Civil Engineering, Environmental and Geodetic Sciences, Koszalin University of Technology, Śniadeckich 2, 75-453 Koszalin, Poland

³Faculty of Civil and Environmental Engineering, Gdansk University of Technology, Gabriela Narutowicza 11/12, 80-233 Gdansk, Poland

*mmatyszewski@cbk.poznan.pl

Abstract

Satellite Laser Ranging (SLR) is a modern technique used in various research areas and applications related to geodesy and geodynamics. It is commonly used for tasks such as establishing the International Terrestrial Reference Frame (ITRF), monitoring Earth Orientation Parameters (EOP), determining the geocenter, measuring fundamental physical constants, calibrating microwave tracking techniques, conducting time transfer experiments, and studying gravitational and general relativistic effects. Laser measurements of the LARES and LAGEOS satellites are used to determine the relativistic effects acting on these satellites. The objective of the present research is to analyze the perturbing forces of relativistic origin (Schwarzschild, de Sitter and Lense-Thirring effects) acting on the LARES, LAGEOS-1 and LAGEOS-2 satellites. By using data from fifteen SLR measurement stations, the precise orbits of these satellites were determined over a span of 840 hours using the GEODYN II orbital software package. The calculation process used a set of procedures, models of forces, and constants that are currently recommended by the International Earth Rotation and Reference Systems Service (IERS) and the International Laser Ranging Service (ILRS). Based on the precise orbits of the LARES, LAGEOS-1, and LAGEOS-2 satellites, calculations were made to determine the values of relativistic accelerations acting on these satellites. These values oscillate with a period equal to half of the orbital period for the de Sitter and Lense-Thirring effects, and a quarter of the orbital period for the Schwarzschild effect.

Key words: Satellite Laser Ranging technique, relativistic accelerations, effects: Schwarzschild, de Sitter and Lense-Thirring, precise orbit determination.

1 Introduction

The movement of artificial satellites in space around Earth is influenced by several perturbing forces. Some forces cause the acceleration of satellites, including the acceleration predicted by the General Theory of Relativity (GTR). These forces include the Schwarzschild

effect, the de Sitter effect (also known as the geodetic precession effect), and the Lense-Thirring effect (also known as the frame-dragging effect), studied in Huang et al. (1990). The International Earth Rotation and Reference Systems Service (IERS) recommends considering these effects for precise orbit determination of satellites (Petit and Luzum, 2010).

In the early 20th century, Karl Schwarzschild solved the Einstein field equations (Schwarzschild, 2003). This solution completely describes the space around a stationary system with matter distributed in a spherical manner around a central point. It predicts that objects in the gravitational field experience relativistic accelerations, which can be described by the following formula (Huang et al., 1990):

$$\vec{a}_{Sch} = \frac{GM}{c^2 r^3} \left[\left[4 \frac{GM}{r} - v^2 \right] \vec{r} + 4 (\vec{v} \cdot \vec{r}) \vec{v} \right] \quad (1)$$

where c is the speed of light in a vacuum, G is the gravitational constant of the Earth, M is the mass of the Earth, r is the distance from the satellite to the center of mass of the Earth, \vec{r} is the geocentric vector of the satellite's position, v is the speed of the satellite and \vec{v} is the geocentric vector of the satellite's speed.

The Dutch mathematician, physicist and astronomer Willem de Sitter was the first person to predict the influence of a vector carried with a body orbiting the curvature of space-time (De Sitter, 1917). He determined the relativistic correction for the Earth-Moon system, which is known as the geodesic precession or the de Sitter effect. It depends on the geometry of the satellite-Earth-Sun system (Sošnica et al., 2021). It is assumed that the de Sitter effect remains nearly constant, with the value of a 10^{-11} m/s² range; and it is determined using the formula (Combrinck, 2010):

$$\vec{a}_{deSitter} = 3 \left[\vec{R} \times \frac{-GM_S \vec{R}}{c^2 R^3} \right] \times \vec{v} \quad (2)$$

where M_S is the mass of the Sun, \vec{R} denotes the barycentric position of the Earth, \vec{R} is the barycentric velocity of the Earth, R is the distance of the Earth from the Sun and \vec{v} is the geocentric velocity vector of the satellite.

The Lense-Thirring effect, which is the third relativistic effect, was described by mathematical equations in a seminal work by J. Lense and H. Thirring at the beginning of the 20th century (Lense and Thirring, 1918). According to the General Theory of Relativity (GTR), the movement of mass has an extra effect on the gravitational field. This effect is similar to the electromagnetic field in electrodynamics and is called the gravitational-magnetic field. This field then applies a rotational force on the objects within it (Ciufolini et al., 2016). This effect can also be described using the following analogy: the central body that is rotating causes the spacetime around it to become distorted, similar to how an object immersed in a thick liquid would behave. This distortion results in the transfer of some of the rotational energy of the central body to the surrounding medium (McCarthy et al., 2015). The Lense-Thirring effect causes an acceleration of approximately 10^{-11} m/s², depending on the altitude of the satellite's orbit (Combrinck, 2010). The following equation describes it (Huang et al., 1990):

$$\vec{a}_{L-T} = 2 \frac{GM}{c^2 r^3} \left[\frac{3}{r^2} (\vec{r} \times \vec{v}) (\vec{r} \cdot \vec{J}) + (\vec{v} \times \vec{J}) \right] \quad (3)$$

where M is the mass of the Earth, r is the distance from the satellite to the center of mass of the Earth, \vec{v} is the geocentric velocity vector of the satellite and \vec{J} is the momentum of Earth per mass unit $|\vec{J}| \simeq 9.8 \cdot 10^8$ m/s² (Petit and Luzum, 2010). The relationship between the acceleration values and the height of circular orbits is discussed in (Hugentobler, 2008). The accelerations caused by the Schwarzschild and Lense Thirring effects decrease significantly by two orders of magnitude as the orbit transitions from a low to a high altitude (by 10^3 km). On the other hand, the accelerations caused by the de Sitter effect remain relatively constant. The Schwarzschild effect primarily acts in the radial directions, while the Lense-Thirring effect does not impact the radial component but instead affects the cross-track direction, resulting in a precession of the orbital plane.

On the other hand, the De Sitter effect heavily relies on the relative geometry between the satellite, the Earth, and the Sun.

Research on the impact of relativistic effects on the movement of artificial satellites has been a topic discussed in the literature for many years, but it still remains an open research problem. The first precise measurements of geodetic precession were made using Lunar Laser Ranging (LLR). These measurements had an uncertainty of approximately 1% according to Dickey et al. (1994), and later an uncertainty of 0.6% according to Williams et al. (2004). In turn, Ciufolini et al. (2017) examined the de Sitter effect on the LARES 2 satellite (Ciufolini et al., 2023). The Lense-Thirring effect was confirmed using the LAGEOS-1 and LAGEOS-2 satellites. The uncertainty for this confirmation was 5% considering all the known errors, and 10% allowing for unknown and unmodelled error sources, as stated by Ciufolini and Pavlis (2004). The Lense-Thirring effect was also examined in the work by Ciufolini et al. (2016) and Lucchesi et al. (2019). They found that the secular Lense-Thirring precession on the Right Ascension of the Ascending Node (RAAN) was approximately 30.67 mas/yr, 31.50 mas/yr, and 118.48 mas/yr for the LAGEOS 1, LAGEOS-2, and LARES satellites, respectively. Additionally, Ciufolini et al. (2019) confirmed this effect with a 2% uncertainty using measurements from the same satellites.

NASA conducted the Gravity Probe B (GP-B) satellite mission to experimentally confirm the theory of gravity. The main goal of the mission was to accurately measure the spacetime frame-dragging effect (Lense-Thirring effect) and geodetic precession (de Sitter effect). The satellite, which was orbiting in a polar orbit at an altitude of 642 km, was equipped with four spherical gyroscopes and a telescope. The gyroscopes were aligned with the distant reference star IM Pegasi using a telescope. Then, the deviation of the gyroscopes' axis from the direction to the reference star was measured. The predicted size of the geodetic precession was 6606.1 mas/yr and the Lense-Thirring effect was predicted to be 39.2 mas/yr. The experimental results showed that the geodetic precession was 6601.8 ± 18.3 mas/yr and the Lense-Thirring effect was 37.2 ± 7.2 mas/yr (Everitt et al., 2015).

The influence of relativistic effects on the change of the GALILEO satellite orbit over a period of 24 hours was investigated in Sošnica et al. (2021). In turn, the exact measurement of the precession of the perigee argument of the LAGEOS-2 orbit was described in Lucchesi and Peron (2010, 2014), obtaining 3306.58 mas/yr as the sum of all relativistic effects. In turn, in Lucchesi (2003), the authors present the value of the precession of the perigee argument for the same satellite caused by the Schwarzschild effect as 3351.95 mas/yr. The magnitude of all relativistic accelerations acting on the LARES and LAGEOS satellites is also presented in the paper Sošnica (2014).

The research in this paper is based on data obtained using the Satellite Laser Ranging (SLR) technique. This technique is commonly used in various research areas and is a part of space geodesy measurement techniques. In simple terms, it involves an accurate measurement of the time it takes for a laser pulse to travel from a ground station to a satellite and back (Seeber, 2003). This allows for the measurement of the distance to the satellite, which is expressed as a unit of time. The distance between the station and the satellite is calculated based on the time it takes for the laser pulse to travel. Equation (4) provides the laser observation equation for the i -th laser measurement of the distance from the reference point of the laser sensor to the satellite's mass center:

$$r_{o,i} = \frac{(\Delta t_i - \Delta cal) c}{2} + \Delta a_i + \Delta CoM - \Delta r - \varepsilon_i \quad (4)$$

where Δt_i is the reading from the time interval counter for the i -th measurement, Δcal is a calibration correction, c is a speed of light, Δa_i is an atmospheric correction for the i -th measurement, ΔCoM is a correction for the center of mass of the satellite, Δr is a range bias of the observation and ε_i is a random deviation for i -th measurement. It is important to note that the relativistic corrections

are also applied to the measured distance in SLR as a free-space signal propagation model (Arnold et al., 2019).

The data obtained using the SLR technique are widely used for various tasks in satellite geodesy and geodynamics, such as determining the coordinates of laser stations (Guo et al., 2018; Lejba and Schillak, 2011; Zelensky et al., 2014), in the study of the gravitational field of the Earth (Brzeziński et al., 2016a; Sośnica et al., 2015), determining the parameters of Earth's orientation (Bloßfeld et al., 2018; Brzeziński et al., 2016b; Gourine, 2012; Shen et al., 2015) and rotation (Bogusz et al., 2015), or studying the phenomenon of tides (Jagoda et al., 2016; Rutkowska and Jagoda, 2010, 2015; Sośnica et al., 2015). The SLR technique also supports GNSS systems (Specht, 2022) and participates in the development of GGOS (Sośnica and Bosy, 2019).

The modern technology of performing laser measurements to satellites allows for precision in determining their orbits in the order of single millimeters (Pearlman et al., 2019b). Therefore, it is necessary to use precise calculation methods that consider any effects that may influence satellite movement. The objective of this study was to determine and analyze the accelerations of relativistic origin that affect the LARES, LAGEOS-1, and LAGEOS-2 satellites. The position and velocity vectors of these satellites were determined every 60 seconds using SLR data in the form of normal points (McCarthy et al., 2015). These data were obtained from fifteen stations over a period of 840 hours. A normal point represents all single observations within a specific interval (bin size). Our script calculated the values of accelerations caused by relativistic effects, specifically Schwarzschild, de Sitter, and Lense-Thirring, using Equations (1), (2), and (3). The research used a different approach to determine relativistic accelerations compared to what is presented in the subject literature. The works Lucchesi (2003); Lucchesi et al. (2019) noted that relativistic effects are known as a relativistic precession of individual elements of the Kepler orbit. The research conducted by Everitt et al. (2015) examines relativistic effects by directly measuring the deviation of the axis of the gyroscopes on board the satellite from the reference direction. In our own research, we use data from the SLR to determine relativistic accelerations at 60-second intervals.

2 Objects and orbital computations

2.1 Satellites

Typical Satellite Laser Ranging satellites are passive objects that have the shape of a sphere and are covered with retro-reflectors. Examples of such satellites include AJISAI, LAGEOS, LARES, STARLETTE, STELLA, and others. They can be divided into two main groups: Medium Earth Orbit (MEO) satellites, e.g. LAGEOS-1 (perigee = 5844 km), LAGEOS-2 (perigee = 5622 km), LARES-2 (perigee = 5896 km); and Low Earth Orbit (LEO) satellites, e.g. AJISAI (perigee = 1485 km), LARES (perigee = 1444 km), STELLA (perigee = 804 km), STARLETTE (perigee = 812 km). The research in the study used data from LAGEOS-1, LAGEOS-2, and LARES satellites, which are shown in Figure 1. The selected physical and orbital parameters of these satellites are summarized in Table 1. We chose these satellites based on two factors: a favorable ratio of the satellite's cross-sectional area to its mass (to minimize the impact of non-gravitational effects) and a large number of measurements (normal points).

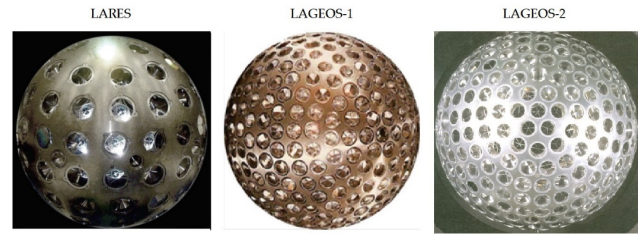


Figure 1. LARES, LAGEOS-1 and LAGEOS-2 satellites

LARES (LAsER Relativity Satellite) (ILRS - LARES, 2023; Pearlman et al., 2019a) was constructed by Agenzia Spaziale Italiana (ASI) and placed in orbit on 13 February 2012. It orbits a low circular orbit with an inclination of 69.5° . It was made from a single layer of metal, more precisely from a high-density tungsten alloy. It was equipped with 92 retro-reflectors, arranged in the form of 10 rings running around the axis of its body. Its ratio of cross-sectional area to mass is the smallest of all other satellites, which also makes it the densest object in the Solar System (Sośnica, 2014). The main objectives of the LARES mission are to enable measurements for the purposes of general relativity, space geodesy, geodynamics; for the very precise determination of the Earth's gravitomagnetic field and the study of the Lense-Thirring effect.

LAGEOS-1 (LAsER GEODYNAMICS Satellite) (ILRS - LAGEOS, 2023; Pearlman et al., 2019a) was launched by NASA on 4 May 1976. The twin of the LAGEOS-1 satellite was created in cooperation between NASA and ASI, and named LAGEOS-2; it was placed in orbit on 22 October 1992. Both satellites circulate in medium orbits with an inclination of 109.8° and 52.6° , respectively. LAGEOS missions are aimed at determining the Earth's reference system, high accuracy Earth Orientation Parameters (EOP) and improving the Earth's gravity field models. They are both made of brass cores covered with aluminum hemispheres. There are 422 retro-reflectors and 4 reflectors made of germanium used for experimental infrared measurements on their surfaces (Sośnica, 2014).

2.2 Orbit determination

The GEODYN II orbital software package (McCarthy et al., 2015) was used to determine the orbits of the LARES, LAGEOS-1, and LAGEOS-2 satellites. The orbits of these satellites were calculated using Cowell's fixed-step method, which involves numerically integrating the equations of motion for the satellites in rectangular coordinates. The calculations followed a set of standard procedures and used force and constant models recommended by the International Earth Rotation and Reference Systems Service (Petit and Luzum, 2010) and the International Laser Ranging Service (Pearlman et al., 2019b). The root mean square of the orbital arc (arc RMS), as defined by Equation (5), is the main parameter used to evaluate the accuracy of the determined orbits:

$$RMS = \sqrt{\frac{\sum_{i=1}^n (O_i - C_i)^2}{n - 1}} \quad (5)$$

where $(O_i - C_i)$ denotes the difference between the observed and calculated distance values, while i denotes the number of SLR data in the form of normal points.

Table 1. Satellites specification

Satellite	Altitude [km]	Inclination [°]	Period [min]	Diameter [cm]	Mass [kg]	Density [g/cm ³]
LAGEOS-1	5850	109.84	225	60	406.965	3.6
LAGEOS-2	5625	52.64	223	60	405.38	3.6
LARES	1450	69.50	115	36	386.8	15.3

Table 2. List of used stations and a number of normal points

No.	Station ID number	Station name, country	Number of normal points
1	7090	Yarragadee, Australia	3093
2	7105	Greenbelt, USA	1645
3	7110	Monument Peak, USA	1476
4	7119	Haleakala, USA	608
5	7237	Changchun, China	776
6	7501	Hartebeesthoek, South Africa	2328
7	7810	Zimmerwald, Switzerland	2861
8	7825	Mt Stromlo, Australia	1048
9	7838	Simosato, Japan	545
10	7839	Graz, Austria	1172
11	7840	Herstmonceux, United Kingdom	1192
12	7841	Potsdam, Germany	1178
13	7845	Grasse, France	290
14	7941	Matera, Italy	2764
15	8834	Wetzell, Germany	1027

Table 3. Obtained RMS and number of normal points for each orbital arc with and without empirical accelerations applied

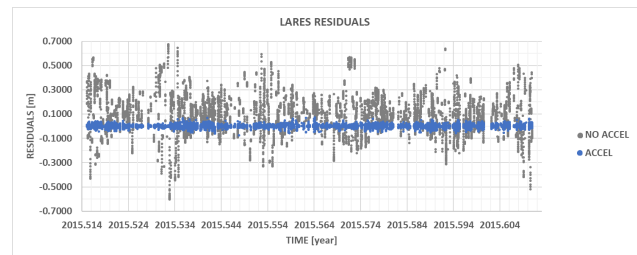
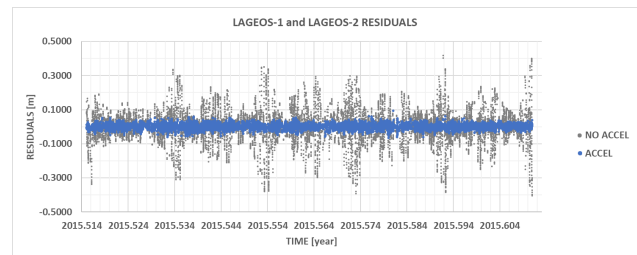
Satellite	Arc number	Number of normal points	RMS with accel [cm]	RMS without accel [cm]
LARES	1	1154	1.38	24.39
	2	1582	1.58	17.38
	3	1149	1.53	19.25
	4	1550	1.53	14.52
	5	1720	1.47	16.05
LAGEOS-1 and LAGEOS-2	1	3045	1.43	6.05
	2	3260	1.52	8.34
	3	2662	1.49	10.04
	4	2878	1.58	8.23
	5	3003	1.28	8.98

The orbits of the studied satellites were determined in the adopted interval of 840 hours with an integration step of 120 seconds for LAGEOS satellites and 30 seconds for LARES. This period was divided into 5 orbital arcs, each with a length of 168 hours. The calculation process was based on SLR measurements in the form of normal points provided by fifteen laser stations. Their breakdown, including the number of normal points, is presented in Table 2.

3 Results and Discussion

This paper presents the results of determining the relativistic accelerations of LAGEOS-1, LAGEOS-2, and LARES satellites caused by the Schwarzschild, de Sitter, and Lense-Thirring effects. The first stage of the research included determining precise orbits (POD) of these satellites.

The RMS values of the post-fit residuals (arc RMS) were used to determine the accuracy of the satellite's orbits. The resulting RMS values of the post-fit residuals, with and without empirical accelerations applied, and the number of normal points for each orbital arc are collected in Table 3. The average RMS of the post-fit residuals, when empirical accelerations are applied, is 1.46 cm for LAGEOS satellites and 1.50 cm for the LARES satellite. Figures 2 and 3 display the obtained residuals from the solution of LARES and LAGEOS orbits, both with and without the use of empirical accelerations. The maximum residual values for the LARES satellite are 0.073 m with empirical accelerations and 0.674 m without them. For the LAGEOS satellites, the maximum residual values are 0.093 m with empirical accelerations and 0.417 m without them. To determine the orbit of the twin satellites LAGEOS, a combined orbit determination approach (LAGEOS-1+LAGEOS-2) was employed.

**Figure 2.** Residuals with and without empirical accelerations applied for LARES satellite**Figure 3.** Residuals with and without empirical accelerations applied for LAGEOS-1 and LAGEOS-2 satellites

This approach is commonly used and results in smaller errors in orbit determination (Schillak et al., 2021; Strugarek et al., 2021).

The orbits of LAGEOS satellites were determined with a slightly greater accuracy. This is because their orbits are located outside the Earth's atmosphere, and the orbits of both satellites were determined together. The orbit of LARES is affected by the Earth's atmosphere and this fact cannot be ignored; it is therefore determined with greater errors than the orbits of the LAGEOS satellites (Ciufolini et al., 2012; Pardini et al., 2017). Another important factor that affects the accuracy of determining the orbit is the number of empirical accelerations used in the computation process. These accelerations are included to account for effects that are not accounted for in the model, which ultimately increases the accuracy of determining the orbit. The GEODYN-II software is capable of applying and solving for general satellite accelerations. These accelerations are determined in three directions: radial, along-track, and cross-track. They also take into account the uncertainties of the assumed model of perturbations. However, we should be cautious when considering the inclusion of empirical acceleration coefficients, as determining these coefficients too frequently may affect the accuracy of the orbital solution (Lucchesi et al., 2019). In this study, empirical accelerations were considered every 84 hours for LAGEOS-1 and LAGEOS-2 satellites, and every 12 hours for the LARES satellite. This is the standard approach used, for example, in Sońnica (2014).

As a result of orbital calculations, precise orbits of LAGEOS and LARES satellites were determined in the form of a set of their positions and velocities in the ECI Cartesian system. The ECI system is a non-rotating, free-falling frame of reference with its origin fixed at the center of the Earth (Ashby, 2004). The positions and velocities of satellites were determined every 60 seconds. In the next stage of the research, these data were used to calculate the acceleration values of the LAGEOS-1, LAGEOS-2, and LARES satellites caused by the effects of Schwarzschild, de Sitter, and Lense-Thirring, respectively, using formulas Equations (1), (2), and (3). We wrote a script in the Octave environment for this purpose. To determine the de Sitter effect, we needed to know the ephemeris of the Earth in the barycentric system of the Sun. To obtain this information, we used the online solar system data calculation service and the JPL Horizons ephemeris provided by the Solar System Dynamics Group from the Jet Propulsion Laboratory (JPL Horizons,

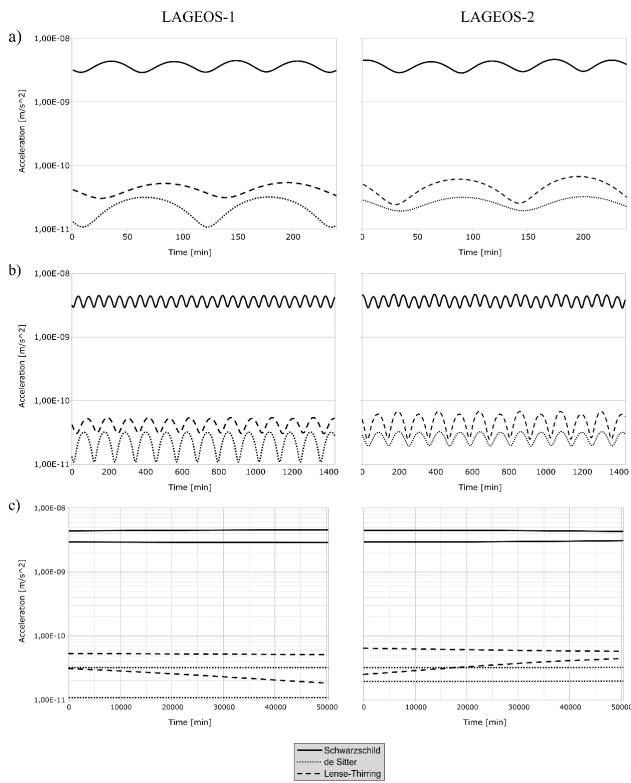


Figure 4. Relativistic accelerations acting on LAGEOS-1 (left column) and LAGEOS-2 (right column) satellites in a 4-hour (a), 24-hour (b) data span correspondingly. Maximum and minimum values of accelerations in 840-hour data span (c)

2023). The data was obtained in the form of a table of position and speed vectors, with a time step of 60 seconds, corresponding to the laser data span used in the POD process.

Figure 4 shows the results of the relativistic accelerations for the LAGEOS-1 and LAGEOS-2 satellites, while Figure 5 shows the results for the LARES satellite. The Figures display the accelerations of Schwarzschild, de Sitter, and Lense-Thirring over different time intervals: 4 hours, 24 hours, and 840 hours, respectively.

Based on the analysis of the results, we noted that the accelerations caused by the Schwarzschild effect are the highest for each satellite. The LARES satellite reaches an average value of $1.40E-8 \text{ m/s}^2$, while the LAGEOS satellites reach an average value of $3.66E-9 \text{ m/s}^2$. The acceleration due to the Lense-Thirring effect is three orders of magnitude lower, averaging $3.67E-11 \text{ m/s}^2$ for LAGEOS-1, $4.65E-11 \text{ m/s}^2$ for LAGEOS-2 and $1.95E-10 \text{ m/s}^2$ for LARES satellite. The acceleration resulting from the de Sitter effect is one order of magnitude smaller than the Lense-Thirring effect for the LARES satellite, averaging $2.54E-11 \text{ m/s}^2$. However, for both LAGEOS satellites, the acceleration is of the same order of magnitude, with an average of $2.00E-11 \text{ m/s}^2$ for LAGEOS-1 and $2.54E-11 \text{ m/s}^2$ for LAGEOS-2. Figures 4 and 5 illustrate that the magnitudes of these accelerations experience short-term oscillations. The specific periods of these oscillations can be found in Table 4.

The accelerations caused by the de Sitter and Lense-Thirring effects have a twice-per-revolution nature for all satellites. Specifically, the LARES satellite experiences these oscillations every 58 minutes, while the LAGEOS satellites have an average period of 112 minutes. On the other hand, the accelerations caused by the Schwarzschild effect have a quadruple-per-revolution nature. The LARES satellite has a period of 28 minutes, while the LAGEOS satellites have an average period of 56 minutes. Figures 4c and 5c display the maximum and minimum acceleration values over the entire 840-hour data span. We observe that the amplitude of these oscil-

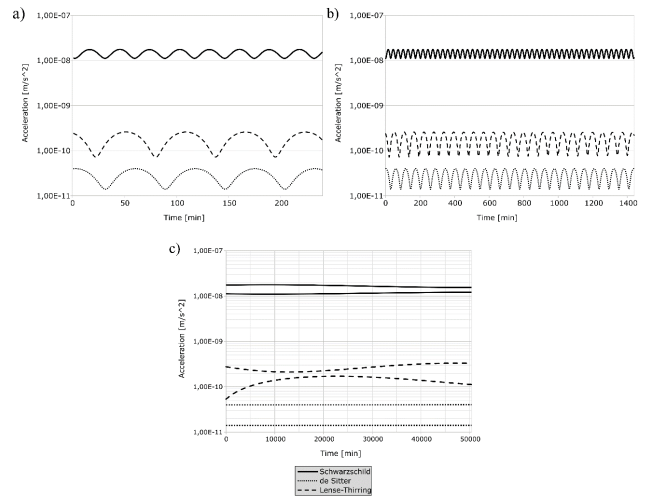


Figure 5. Relativistic accelerations acting on LARES satellite in a 4-hour (a), 24-hour (b) data span correspondingly. Maximum and minimum values of accelerations in 840-hour data span (c)

Table 4. Period of relativistic accelerations oscillations acting on LARES and LAGEOS satellites

Relativistic effects	Period of relativistic acceleration oscillations [min]		
	LARES	LAGEOS-1	LAGEOS-2
Schwarzschild	28	55 – 58	55 – 57
De Sitter	57	112	110 – 112
Lense-Thirring	58	112	109 – 114

lations varies for the Schwarzschild and Lense-Thirring effects.

However, for the de Sitter effect, this amplitude is constant, because in this case the magnitude of accelerations depends on the relative position and speed of the satellite-Earth-Sun system (Sońnica et al., 2021).

Table 5 presents the average acceleration values of relativistic origin for the LARES, LAGEOS-1, and LAGEOS-2 satellites, along with the discrepancies compared to the values reported in Sońnica (2014). Overall, these values are consistent. The highest amplitudes of the determined accelerations are found for the accelerations caused by the Schwarzschild effect for both the LARES satellite and the LAGEOS satellites. Specifically, the acceleration for the LARES satellite is $0.34E-8 \text{ m/s}^2$, for the LAGEOS-1 satellite it is $0.90E-9 \text{ m/s}^2$, and for the LAGEOS 2 satellite it is $0.91E-9 \text{ m/s}^2$. The acceleration amplitudes caused by the de Sit-

Table 5. Values of relativistic accelerations acting on LARES and LAGEOS satellites

Effects	Mean values of relativistic accelerations obtained in this paper [m/s^2]		
	LARES	LAGEOS-1	LAGEOS-2
Schwarzschild	$1.40E-8$	$3.66E-9$	$3.67E-9$
De Sitter	$2.54E-11$	$2.00E-11$	$2.54E-11$
Lense-Thirring	$1.95E-10$	$3.67E-11$	$4.65E-11$
Effects	Differences between the obtained values and those presented in (Sońnica, 2014) [m/s^2]		
	LARES	LAGEOS-1	LAGEOS-2
Schwarzschild	$0.30E-8$	$0.86E-9$	$0.87E-9$
De Sitter	$1.66E-11$	$1.40E-11$	$0.86E-11$
Lense-Thirring	$0.55E-10$	$0.97E-11$	$1.95E-11$

Table 6. Mean and standard deviation of errors of determined relativistic accelerations

Relativistic effects		LARES	LAGEOS-1	LAGEOS-2
Schwarzschild	Mean	2.92E-12	3.15E-14	4.03E-14
	Standard deviation	4.71E-12	2.66E-14	3.29E-14
de Sitter	Mean	1.72E-15	1.11E-16	8.56E-17
	Standard deviation	1.22E-15	4.10E-17	3.62E-17
Lense-Thirring	Mean	3.84E-14	2.46E-16	5.22E-16
	Standard deviation	6.17E-14	2.44E-16	5.27E-16

ter effect are $1.32\text{E-}11\text{ m/s}^2$ for the LARES satellite, $1.08\text{E-}11\text{ m/s}^2$ for the LAGEOS-1 satellite, and $0.67\text{E-}11\text{ m/s}^2$ for the LAGEOS-2 satellite. The acceleration amplitudes caused by the Lense-Thirring effect are $1.31\text{E-}10\text{ m/s}^2$ for the LARES satellite, $1.80\text{E-}11\text{ m/s}^2$ for the LAGEOS-1 satellite, and $2.16\text{E-}11\text{ m/s}^2$ for the LAGEOS-2 satellite. The differences that are observed are a result of the calculation process and the specific conditions that were used. These conditions include the length of the orbital arcs that were considered, the number of normal points used in the calculations, the selection of SLR stations based on the available data, the force models that were applied, and the specific parameters that were used. The errors and standard deviations for the obtained accelerations were determined. The mean error values and their deviation are presented in Table 6.

4 Summary

The research presented in this paper used the Satellite Laser Ranging technique to determine accelerations caused by relativistic effects. The results obtained from this method are consistent with the results found in existing literature. In the literature, these effects are either modeled as a precession of the object's orbit or directly measured as a deviation of the gyroscopes on the satellite from the reference direction. The results of the conducted research show that the average acceleration values caused by the Schwarzschild, de Sitter and Lense-Thirring effects for the LARES satellite are as follows: $1.40\text{E-}8\text{ m/s}^2$, $2.54\text{E-}11\text{ m/s}^2$, $1.95\text{E-}10\text{ m/s}^2$; for the LAGEOS-1 satellite they are: $3.66\text{E-}9\text{ m/s}^2$, $2.00\text{E-}11\text{ m/s}^2$, $3.67\text{E-}11\text{ m/s}^2$ and for the LAGEOS-2 satellite they are: $3.67\text{E-}9\text{ m/s}^2$, $2.54\text{E-}11\text{ m/s}^2$, $4.65\text{E-}11\text{ m/s}^2$. The results obtained confirm that the accelerations of relativistic origin have a periodic nature. These accelerations oscillate with a period equal to half of the orbital period for the de Sitter and Lense-Thirring effects. For the LARES satellite, this period is 58 minutes, and for the LAGEOS satellites, it is on average 112 minutes. For the Schwarzschild effect, the period is a quarter of the orbital period, which is 28 minutes for the LARES satellite and on average 56 minutes for the LAGEOS satellites. The amplitude of oscillation remains constant throughout the studied interval only for accelerations caused by the de Sitter effect. Laser measurements of the LARES and LAGEOS satellites allow to determine the relativistic effects acting on these satellites.

Determining the accelerations caused by relativistic effects is a complex task that requires a meticulous approach and ongoing research into non-gravitational perturbations. These perturbations impact satellites like LAGEOS and LARES. Secular changes in the Keplerian parameters can be identified by analyzing long time series of osculating parameters. However, small accelerations of the magnitude $1\text{E-}10$ or $1\text{E-}11\text{ m/s}^2$ cannot be directly detected through SLR measurements. Additional efforts are needed to enhance dynamic models that accurately describe intricate phenomena such as satellite spin, resistance from the neutral atmosphere (particularly important for the LARES satellite), the Yarkovsky-Schach thermal effect, and the Earth-Yarkovsky effect.

References

- Arnold, D., Montenbruck, O., Hackel, S., and Sośnica, K. (2019). Satellite laser ranging to low Earth orbiters: orbit and network validation. *Journal of geodesy*, 93(11):2315–2334, doi:10.1007/s00190-018-1140-4.
- Ashby, N. (2004). The Sagnac effect in the Global Positioning System. In Rizzi, G. and Ruggiero, M. L., editors, *Relativity in rotating frames: relativistic physics in rotating reference frames*, pages 11–28. Springer.
- Bloßfeld, M., Rudenko, S., Kehm, A., Panafidina, N., Müller, H., Angermann, D., Hugentobler, U., and Seitz, M. (2018). Consistent estimation of geodetic parameters from SLR satellite constellation measurements. *Journal of Geodesy*, 92:1003–1021, doi:10.1007/s00190-018-1166-7.
- Bogusz, J., Brzezinski, A., Kosek, W., and Nastula, J. (2015). Earth rotation and geodynamics. *Geodesy and Cartography*, 64(2), doi:10.1515/geocart-2015-0013.
- Brzeziński, A., Barlik, M., Andrasik, E., Izdebski, W., Kruczyk, M., Liwosz, T., Olszak, T., Pachuta, A., Pieniak, M., Próchniewicz, D., Rajner, M., Szpunar, R., Tercjak, M., and Walo, J. (2016a). Geodetic and geodynamic studies at Department of Geodesy and Geodetic Astronomy WUT. *Reports on Geodesy and Geoinformatics*, 100(1):165–200, doi:10.1515/rgg-2016-0013.
- Brzeziński, A., Jóźwik, M., Kaczorowski, M., Kalarus, M., Kasza, D., Kosek, W., Nastula, J., Szczerbowski, Z., Wińska, M., Wronowski, R., Zdunek, R., and Zieliński, J. B. (2016b). Geodynamic research at the Department of Planetary Geodesy, SRC PAS. *Reports on Geodesy and Geoinformatics*, 100(1):131–147, doi:10.1515/rgg-2016-0011.
- Ciufolini, I., Matzner, R., Gurzadyan, V., and Penrose, R. (2017). A new laser-ranged satellite for General Relativity and space geodesy: III. De Sitter effect and the LARES 2 space experiment. *The European Physical Journal C*, 77:1–6, doi:10.1140/epjc/s10052-017-5339-y.
- Ciufolini, I., Paolozzi, A., Pavlis, E., Ries, J., Gurzadyan, V., Koenig, R., Matzner, R., Penrose, R., and Sindoni, G. (2012). Testing General Relativity and gravitational physics using the LARES satellite. *The European Physical Journal Plus*, 127:1–7, doi:10.1140/epjp/i2012-12133-8.
- Ciufolini, I., Paolozzi, A., Pavlis, E. C., Koenig, R., Ries, J., Gurzadyan, V., Matzner, R., Penrose, R., Sindoni, G., Paris, C., Khachatryan, H., and Mirzoyan, S. (2016). A test of general relativity using the LARES and LAGEOS satellites and a GRACE Earth gravity model: Measurement of Earth's dragging of inertial frames. *The European Physical Journal C*, 76:1–7, doi:10.1140/epjc/s10052-016-3961-8.
- Ciufolini, I., Paolozzi, A., Pavlis, E. C., Sindoni, G., Ries, J., Matzner, R., Koenig, R., Paris, C., Gurzadyan, V., and Penrose, R. (2019). An improved test of the general relativistic effect of frame-dragging using the LARES and LAGEOS satellites. *The European Physical Journal C*, 79(10):872, doi:10.1140/epjc/s10052-019-7386-z.
- Ciufolini, I., Paris, C., Pavlis, E. C., Ries, J., Matzner, R., Paolozzi, A.,

- Ortore, E., Bianco, G., Kuzmicz-Cieslak, M., Gurzadyan, V., et al. (2023). First results of the LARES 2 space experiment to test the general theory of relativity. *The European Physical Journal Plus*, 138(11):1054, doi:10.1140/epjp/s13360-023-04696-6.
- Ciufolini, I. and Pavlis, E. C. (2004). A confirmation of the general relativistic prediction of the Lense-Thirring effect. *Nature*, 431(7011):958–960, doi:10.1038/nature03007.
- Combrinck, L. (2010). Satellite Laser Ranging. In Xu, G., editor, *Sciences of Geodesy – I*, pages 301–338. Springer, doi:10.1007/978-3-642-11741-1_9.
- De Sitter, W. (1917). Einstein's theory of gravitation and its astronomical consequences. Third paper. *Monthly Notices of the Royal Astronomical Society*, 78:3–28, doi:10.1093/mnras/78.1.3.
- Dickey, J. O., Bender, P., Faller, J., Newhall, X., Ricklefs, R., Ries, J., Shelus, P., Veillet, C., Whipple, A., Wiant, J., Williams, J. G., and Yoder, C. F. (1994). Lunar Laser Ranging: A continuing legacy of the Apollo Program. *Science*, 265(5171):482–490, doi:10.1126/science.265.5171.482.
- Everitt, C., Muhlfelder, B., DeBra, D., Parkinson, B., Turneure, J., Silbergleit, A., Acworth, E., Adams, M., Adler, R., Bencze, W., et al. (2015). The Gravity Probe B test of general relativity. *Classical and Quantum Gravity*, 32(22):224001, doi:10.1088/0264-9381/32/22/224001.
- Gourine, B. (2012). Use of Starlette and LAGEOS-1&-2 laser measurements for determination and analysis of stations coordinates and EOP time series. *Comptes Rendus Geoscience*, 344(6-7):319–333, doi:10.1016/j.crte.2012.05.002.
- Guo, J., Wang, Y., Shen, Y., Liu, X., Sun, Y., and Kong, Q. (2018). Estimation of SLR station coordinates by means of SLR measurements to kinematic orbit of LEO satellites. *Earth, Planets and Space*, 70(1):201, doi:10.1186/s40623-018-0973-7.
- Huang, C., Ries, J., Tapley, B., and Watkins, M. (1990). Relativistic effects for near-earth satellite orbit determination. *Celestial Mechanics and Dynamical Astronomy*, 48:167–185, doi:10.1007/BF00049512.
- Hugentobler, U. (2008). Orbit perturbations due to relativistic corrections. Unpublished notes available at https://impacts.obspm.fr/content/supporting_material/chapter10/relativity_hugentobler.pdf.
- ILRS - LAGEOS (2023). International Laser Ranging Service, LAGEOS-1,-2. Official Website of ILRS. Last accessed January 2023.
- ILRS - LARES (2023). International Laser Ranging Service, LARES - LAsER RELativity Satellite. Official Website of ILRS. Last accessed January 2023.
- Jagoda, M., Rutkowska, M., and Kraszewska, K. (2016). The evaluation of time variability of tidal parameters h and l using SLR technique. *Acta Geodynamica et Geomaterialia*, 14(2):153–158, doi:10.13168/AGG.2016.0036.
- JPL Horizons (2023). Jet Propulsion Laboratory Horizons System. Official Website of JPL. Last accessed January 2023.
- Lejba, P. and Schillak, S. (2011). Determination of station positions and velocities from laser ranging observations to Ajisai, Starlette and Stella satellites. *Advances in Space Research*, 47(4):654–662, doi:10.1016/j.asr.2010.10.013.
- Lense, J. and Thirring, H. (1918). Über den einfluss der eigenrotation der zentralkörper auf die bewegung der planeten und monde nach der einsteinschen gravitationstheorie. *Physikalische Zeitschrift*, 19:156.
- Lucchesi, D. M. (2003). LAGEOS II perigee shift and Schwarzschild gravitoelectric field. *Physics Letters A*, 318(3):234–240, doi:10.1016/j.physleta.2003.07.015.
- Lucchesi, D. M., Anselmo, L., Bassan, M., Magnafico, C., Pardini, C., Peron, R., Pucacco, G., and Visco, M. (2019). General relativity measurements in the field of earth with Laser-Ranged satellites: state of the art and perspectives. *Universe*, 5(6):141, doi:10.3390/universe5060141.
- Lucchesi, D. M. and Peron, R. (2010). Accurate measurement in the field of the earth of the general-relativistic precession of the LAGEOS II pericenter and new constraints on non-newtonian gravity. *Physical Review Letters*, 105(23):231103, doi:10.1103/PhysRevLett.105.231103.
- Lucchesi, D. M. and Peron, R. (2014). LAGEOS II pericenter general relativistic precession (1993–2005): Error budget and constraints in gravitational physics. *Physical Review D*, 89(8):082002, doi:10.1103/PhysRevD.89.082002.
- McCarthy, J., Rowton, S., Moore, D., Pavlis, D., Luthcke, S., and Tsaoussi, T. (2015). GEODYN systems description, volume 1. Technical report.
- Pardini, C., Anselmo, L., Lucchesi, D., and Peron, R. (2017). On the secular decay of the LARES semi-major axis. *Acta Astronautica*, 140:469–477, doi:10.1016/j.actaastro.2017.09.012.
- Pearlman, M., Arnold, D., Davis, M., Barlier, F., Biancale, R., Vasilev, V., Ciufolini, I., Paolozzi, A., Pavlis, E. C., Sośnica, K., and Blossfeld, M. (2019a). Laser geodetic satellites: a high-accuracy scientific tool. *Journal of Geodesy*, 93:2181–2194, doi:10.1007/s00190-019-01228-y.
- Pearlman, M. R., Noll, C. E., Pavlis, E. C., Lemoine, F. G., Combrinck, L., Degnan, J. J., Kirchner, G., and Schreiber, U. (2019b). The ILRS: approaching 20 years and planning for the future. *Journal of Geodesy*, 93:2161–2180, doi:10.1007/s00190-019-01241-1.
- Petit, G. and Luzum, B. (2010). IERS Technical Note No. 36. Technical report, Bureau International Des Poids Et Mesures Sevres (France), 1–179.
- Rutkowska, M. and Jagoda, M. (2010). Estimation of the elastic Earth parameters (h2, l2) using SLR data. *Advances in space research*, 46(7):859–871, doi:10.1016/j.asr.2010.04.010.
- Rutkowska, M. and Jagoda, M. (2015). SLR technique used for description of the Earth elasticity. *Artificial Satellites*, 50(3):127–141, doi:10.1515/arsa-2015-0010.
- Schillak, S., Lejba, P., and Michałek, P. (2021). Analysis of the quality of SLR station coordinates determined from Laser Ranging to the LARES satellite. *Sensors*, 21(3):737, doi:10.3390/s21030737.
- Schwarzschild, K. (2003). On the gravitational field of a mass point according to Einstein's theory. *Gen. Relativ. Gravit.*, 35(5):951–959, doi:10.1023/A:1022971926521.
- Seeber, G. (2003). *Satellite geodesy, 2nd ed.* Walter de gruyter, doi:10.1515/9783110200089.
- Shen, Y., Guo, J., Zhao, C., Yu, X., and Li, J. (2015). Earth rotation parameter and variation during 2005–2010 solved with LAGEOS SLR data. *Geodesy and Geodynamics*, 6(1):55–60, doi:10.1016/j.geog.2014.12.002.
- Sośnica, K. (2014). *Determination of precise satellite orbits and geodetic parameters using Satellite Laser Ranging.* Astronomical Institute, University of Bern, Switzerland, doi:10.7892/boris.53915.
- Sośnica, K. and Bosy, J. (2019). Global Geodetic Observing System 2015–2018. *Advances in Geodesy and Geoinformation*, 68(1):121–144, doi:10.24425/gac.2019.126090.
- Sośnica, K., Bury, G., Zajdel, R., Kazmierski, K., Ventura-Traveset, J., Prieto-Cerdeira, R., and Mendes, L. (2021). General relativistic effects acting on the orbits of Galileo satellites. *Celestial Mechanics and Dynamical Astronomy*, 133:14, doi:10.1007/s10569-021-10014-y.
- Sośnica, K., Jäggi, A., Meyer, U., Thaller, D., Beutler, G., Arnold, D., and Dach, R. (2015). Time variable Earth's gravity field from SLR satellites. *Journal of Geodesy*, 89:945–960, doi:10.1007/s00190-015-0825-1.
- Specht, M. (2022). Experimental studies on the relationship between HDOP and position error in the GPS system. *Metrology and Measurement Systems*, 29(1):17–36, doi:10.24425/mms.2022.138549.
- Strugarek, D., Sośnica, K., Arnold, D., Jäggi, A., Zajdel, R., and Bury, G. (2021). Determination of SLR station coordinates based on LEO, LARES, LAGEOS, and Galileo satellites. *Earth, Planets and Space*, 73:87, doi:10.1186/s40623-021-01397-1.
- Williams, J. G., Turyshev, S. G., and Boggs, D. H. (2004). Progress in

lunar laser ranging tests of relativistic gravity. *Physical Review Letters*, 93(26):261101, [doi:10.1103/PhysRevLett.93.261101](https://doi.org/10.1103/PhysRevLett.93.261101).
Zelensky, N. P., Lemoine, F. G., Chinn, D. S., Melachroinos, S., Beckley, B. D., Beall, J. W., and Bordyugov, O. (2014). Estimated SLR

station position and network frame sensitivity to time-varying gravity. *Journal of Geodesy*, 88:517–537, [doi:10.1007/s00190-014-0701-4](https://doi.org/10.1007/s00190-014-0701-4).